Exp Brain Res (2005) 162: 145–154
DOI 10.1007/s00221-004-2122-8

RESEARCH ARTICLE

H. Hicheur · S. Vieilledent · M. J. E. Richardson · T. Flash · A. Berthoz

Velocity and curvature in human locomotion along complex curved paths: a comparison with hand movements

Received: 18 December 2003 / Accepted: 13 September 2004 / Published online: 7 December 2004

Abstract There is extensive experimental evidence linking instantaneous velocity to curvature in drawing and hand-writing movements. The empirical relationship between these characteristics of motion and path is well described by a power law in which the velocity varies in proportion to the one-third power of the radius of curvature. It was recently shown that a similar relationship can be observed during locomotion along curved elliptical paths raising the possibility that these very different motor activities might, at some level, share the same planning strategies. It has, however, been noted that the ellipse is a special case with respect to the one-third power law and therefore these previous results might not provide strong evidence that the one-third power law is a general feature of locomotion around curved paths. For this reason the experimental study of locomotion and its comparison with hand writing is extended here to non-elliptical paths. Subjects walked along predefined curved paths consisting of two complex shapes drawn on the ground: the cloverleaf and the limacon. It was found that the data always supported a close relationship between instantaneous velocity and curvature. For these more complex paths, however, the relationship is shape-dependent—although velocity and curvature can still be linked by a power law, the exponent depends on the geometrical form of the path. The results demonstrate the existence of a close relationship between instantaneous velocity and curvature in locomotion that is more general than the one-third power law. The origins of this relationship and its possible explanation in the mechanical balance of forces and in central planning are discussed.

Keywords Locomotion · Curved paths · Whole body · Kinematics · Geometry

H. Hicheur (✉) · S. Vieilledent · M. J. E. Richardson · A. Berthoz
Laboratoire de Physiologie de la Perception et de l'Action,
CNRS Collège de France,
11 place Marcelin Berthelot,
75005 Paris, France
e-mail: halim.hicheur@college-de-france.fr
Tel.: +33-1-44-27-14-07
Fax: +33-1-44-27-13-82

H. Hicheur
Laboratoire Mouvement Action et Performance, INSEP,
75012 Paris, France

T. Flash
Department of Applied Mathematics, Weizmann Institute of Science,
76200 Rehovot, Israel

Present address:
S. Vieilledent
CURAPS, Université de la Réunion,
97430 Le Tampon, France

Present address:
M. J. E. Richardson
Laboratory of Computational Neuroscience, École Polytechnique Fédérale de Lausanne,
1015 Lausanne, Switzerland

Introduction

Walking is a motor activity that combines continuous, fine coordination of the limbs and trunk across each step with the planning strategies of goal-directed movements. Walking along curved paths is a common task for humans and puts a greater demand on balance maintenance and motion planning than walking in a straight line. Sensory information coming from different modalities (visual, vestibular, or proprioceptive) is available to the walker for steering in the desired direction. The relative importance of these sources of information has been extensively studied to determine the extent to which they are used in the control of locomotion. Studies on curved locomotion in particular have concentrated on sensory systems which play a role in maintaining stable displacement and gaze control (Grasso et al. 1996; Imai et al. 2001; Courtine and Schieppati 2003). Interactions between the relative movements of the head, body, and eyes have been described (Grasso et al. 1998), and Imai et al. (2001) have drawn attention to the sum of linear accelerations acting on the

head—the so-called gravito inertial acceleration (GIA) vector. The authors proposed that these linear inertial forces underlie the perception of our own movement and help to coordinate the head, body, and eyes when walking along a curved path. These studies, therefore, addressed the vestibular contribution to the control of locomotion along curved paths.

Other approaches have emphasized the role played by visual input in the control of locomotion and the perception of displacement in the environment. For example, when walking toward a specific location (locomotor goal) a person might displace his body by trying to minimize the variations between the heading (perceived from optic flow) and the goal, by placing the focus of expansion on the target (Warren et al. 2001). Alternatively, a person might perceive the visual direction of the goal with respect to the body and walk in this direction, centring the goal at the midline with respect to the body's locomotor axis. These two strategies have been addressed in the context of locomotion along straight-line paths (Warren et al. 2001). In contrast Wilkie and Wann (2003) proposed that it might not be necessary to recover heading from optic flow in the control of curved locomotion. Rather they emphasized the role of active gaze and retinal flow (or extra retinal gaze angle information) for the control of steering around curved paths.

These approaches have emphasized the vestibular (Imai et al. 2001) and visual contributions in the on-line control of locomotion (Warren et al. 2001; Wilkie and Wann 2003). Few studies have been designed to study the relationship between locomotor velocity and the local curvature of the locomotor path or have addressed the effect of the trajectory as a whole on locomotor planning. This analysis of dynamic and static features of goal-directed movements along desired paths has, however, been one of the central approaches in the study of arm control.

Curved hand trajectories: the one-third power law

A striking characteristic of human arm trajectories is that they show a stereotyped velocity profile when the path is constrained (for point to point movements or the tracing of a template) both in terms of position and velocity (Abend et al. 1982). It is still not clear which criteria are employed by the central nervous system (CNS) to generate such repetitive patterns. For example, many authors have considered the maximization of smoothness of the endpoint trajectories as an optimisation criterion, achieved either by the minimization of the hand jerk (Flash and Hogan 1985) or by the minimization of the rate of change of joint torques (Kawato et al. 1990). The stereotypic patterns observed in human arm trajectories might be the product of several simplifying rules governing arm trajectory formation. One of these rules manifests itself in a relationship between geometrical and kinematic attributes of the trajectories observed for 2D (Viviani and Terzuolo 1982) and 3D (Massey et al. 1992; Cheron et al. 1999) human handwriting and drawing movements. According to this relationship (Eqs 1 and 2), hand velocity decreases at the more curved parts of the trajectory and increases when the trajectory becomes straighter. A power law relating tangential velocity to the radius of curvature was introduced in order to describe how the CNS might generate and control these movements (Lacquaniti et al. 1983), and is expressed as follows:

$$V(t) = K.R(t)^{\beta} \tag{1}$$

or, equivalently, in the logarithmic form:

$$\log V(t) = \log K + \beta.\log R(t) \tag{2}$$

where V is the hand tangential velocity, R is the radius of curvature, β is a constant exponent, and K is the *velocity gain factor*, which is a piecewise constant (Viviani and Cenzato 1985). For complex trajectories these authors showed that the velocity gain factor K is constant within some identifiable geometrical subunits and discontinuously changes at the transition points that separate two consecutive units. This observation, of identifiable units of motor action, suggests a segmentation strategy for the planning of complex movements. Although K changes from one unit to another, the β exponent was empirically found to be near 1/3 for all parts of the trajectory. Thus the one-third power law provides a quantitative description of both movement generation and segmentation.

The mechanisms that lie at the origin of this law are still debated. Schaal and Sternad (2001) have proposed that the nonlinear properties of mechanical systems such as the arm may contribute significantly to the observation of the law. The same authors (Sternad and Schaal 1999) have also proposed that, rather than reflecting a segmented control mechanism, the modulation of the velocity gain factor K is merely a by product of the underlying mechanics. At the same time that the hand appears to undergo discontinuous changes in the velocity gain factor, analysis of joint angles showed only continuous oscillatory patterns without the necessity for the CNS to modulate a specific term K—the apparent discontinuities come from the non-linear relationship of joints to hand position. Wann et al. (1988) were able to predict this power law for elliptical drawing movements after modification of the original minimum-jerk model where they replaced the assumption of a Newtonian point-mass with a visco-elastic body and in a related study Gribble and Ostry (1996) showed that the spring-like properties of the arm might contribute significantly to the emergence of the power law. The conclusion of these authors is that this power law is a by-product of muscle mechanics and has no central origins.

Other computational models based on optimality principles such as maximum smoothness (Todorov and Jordan 1998; Richardson and Flash 2002) or minimum variance (Harris and Wolpert 1998) also predict the one-third power law. These results suggest that the law might

be an epiphenomenon of a particular global planning strategy.

In contrast, many studies have claimed that the power is centrally planned. For example, de'Sperati and Viviani (1997) have found that the power law applies also to pursuit eye movements. Recent neurophysiological observations provided a neural correlate to this law. In a drawing task where monkeys traced curved paths (lemniscates or ellipses), Schwartz and coworkers showed that the power law described for human drawing was also evident in the neural representation of monkey hand trajectories (Schwartz and Moran 1999; Reina and Schwartz 2003). These authors studied the magnitude of population vectors calculated from firing rates of large populations of cells in the motor cortex while the monkeys were drawing. They found that a relationship between the directional and speed representation in the firing rates of these cells is robust during drawing. Moreover the power law was represented in both the neural (the time-shifted population vectors; see Schwartz and Moran 1999 for details) and actual hand trajectories leading the authors to the conclusion that the one-third power law is a direct product of neural processing.

Regardless of whether the observed power law is caused by peripheral mechanisms, central mechanisms, or some combination thereof, it is nevertheless a succinct representation of an experimentally robust feature of hand drawing movements.

The one third power law in human locomotion

Recently, the relationship between velocity and curvature was examined for human locomotion (Vieilledent et al. 2001). The same form of relationship between velocity and radius of curvature was found—during locomotor movement along elliptical paths the 2D head motion obeyed the one-third power law. This observation did not depend either on the direction of walking (clockwise or counter clockwise) or on the walking speed being tested (normal and fast). It should be noted that the power law has also been observed during locomotion at the level of the foot trajectory (Ivanenko et al. 2002). Concerning the ellipses used by Vieilledent et al. (2001) it has been argued that, from the standpoint of the power law, ellipses are a special case and do not provide a stringent test—power-law motion around an ellipse corresponds to simple harmonic motion. It is therefore necessary to test locomotion around more complex paths to assess the robustness of this power law for whole-body displacement during human locomotion. This is the purpose of the current study.

The aim is to examine the relationship between velocity and curvature at the level of the displacement of the body as a whole around two complex shapes—the cloverleaf and the limacon—that have already been studied for hand drawing (Viviani and Flash 1995). Because these shapes are constituted of separable geometrical units this allows us to also test for a constancy or modulation of the velocity gain factor K (as reported for hand movements) at the transition points separating some specific portions of the trajectory. Results will systematically be compared with those observed by Viviani and Flash (1995) to examine the common and distinct features of the planning strategies for hand motion and full-body displacement around the similar shapes.

Methods

Procedure

The tested paths consisted of a cloverleaf (Fig. 1) and a limacon both, with a perimeter of 20 meters. They were drawn on the floor before the experiment using their parametric coordinates (Viviani and Flash 1995) according to the following equations:

Cloverleaf (Eq. 3)	Limacon (Eq. 4)
$\begin{cases} X(\theta) = a.\sin 2\theta.\cos\theta \\ Y(\theta) = a.\sin 2\theta.\sin\theta \end{cases}$	$\begin{cases} X(\theta) = a.(\cos\theta + b.\cos 2\theta) \\ Y(\theta) = c.(\sin\theta + b.\sin 2\theta) \end{cases}$
With	With
a=2.06 m	a=0.88 m,b=2.42, and c=0.36 m

Task

Nine male subjects (age 32.1±11.8 years) with no known visual or vestibular pathology volunteered for the experiment. The experiments were approved by the local ethics committee and subjects gave their informed consent before their inclusion in the study. Each subject was required first to observe the path drawn on the floor and then to walk

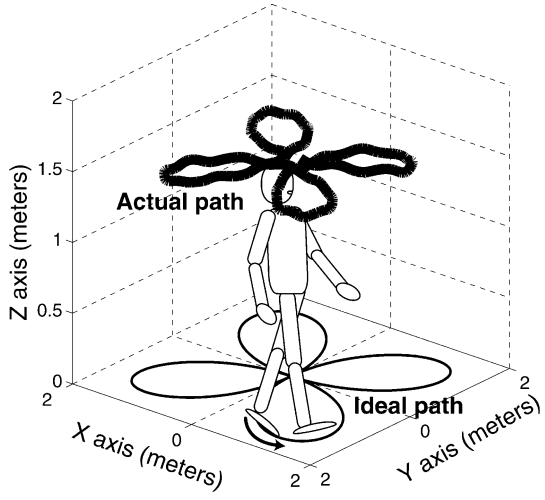

Fig. 1 Subjects walked along a twenty-meter perimeter shape drawn on the ground (here the cloverleaf) in a counter-clockwise direction (*arrow*). Each subject walked five consecutive laps, with the analysis focusing on the laps 2, 3, and 4. The body marker corresponds to the midpoint of the shoulders

accurately at normal ("natural") velocity along it. They performed three trials for the two shapes (cloverleaf and limacon). Each trial comprised five consecutive complete revolutions of the shape (laps) in a counter-clockwise direction (CCW) at a velocity comfortable for the subject. If subjects deviated significantly from the shape drawn on the ground the trial was rejected. Within a trial we isolated the second, third and fourth completion and treated them separately in a lap by lap analysis. Furthermore, each lap of the limacon was split into two loops corresponding to the small and large parts of the shape. Thus, we analysed for each subject 3 trials×2 shapes×3 laps where each lap of the cloverleaf was regarded as a single loop and each lap of the limacon contained two loops, one big and one small.

Headphones providing white noise were worn to prevent any focusing by the subject on auditory cues or the counting of steps. Light-reflective markers were located on the body (left and right shoulders) of the subjects. The 3D positions of these markers in space were recorded at a sampling rate of 60 Hz using an optoelectronic video motion capture device (Vicon V8, Oxford Metrics) composed of 13 cameras. The midpoint of the line joining the left and right shoulder markers was taken as the position of the body in space. It is the X,Y recorded positions which are used to calculate the trajectory and path (Fig. 2). Reconstruction and processing of data were performed using Vicon (Workstation V4.4, Oxford Metrics) and 3DVL software (Kihopsys).

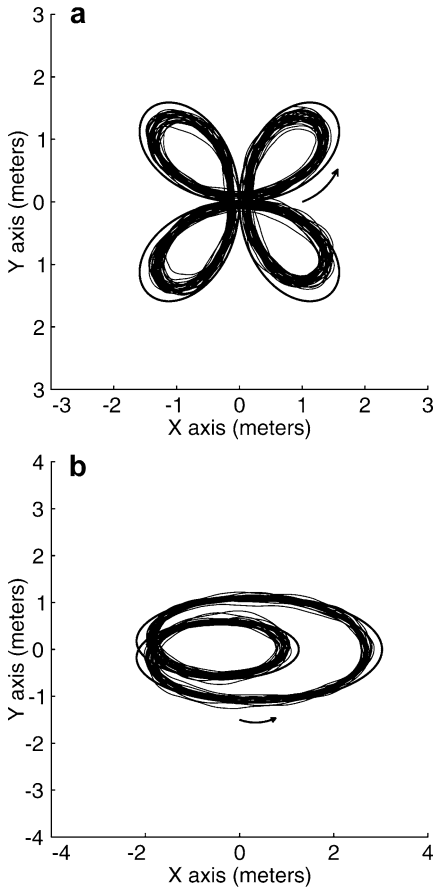

Fig. 2 Trajectories of the body marker projected on to the ground for all subjects (*dark line*) and ideal shape drawn on the ground (*clean line*). The *arrow* indicates the direction of the walk. Note that the trajectories are almost always inside the shape to be followed at the regions of highest curvature. *Top panel*, cloverleaf; *bottom panel*, limacon

Data analysis

Raw data

Data filtering is known to influence the measured velocity–radius relationship for movements of the upper limb (Gribble and Ostry 1996; Schaal and Sternad 2001). In this study raw data was first weakly filtered using a fourth-order low-pass filter algorithm with a high cut-off frequency of 10.0 Hz.

Velocity profile

Human walking is characterized by velocity oscillations, because of the pendular mechanical energy exchange between the potential and kinetic energies (Cavagna and Margaria 1966). These oscillations are observed within each step and depend on walking speed (Willems et al. 1995). The present study focuses on the influence of the geometry of the curved locomotor path and velocity profile calculated in the horizontal plane (the duration for a complete revolution of the trajectory is equal, at least, to 12 s) at the level of the shape as whole. The higher-frequency stepping oscillations were therefore effectively averaged out by further filtering the velocity profile using the same filtering algorithm, but with a cut-off frequency of 0.5 Hz.

Curvature profile

In order to calculate the velocity–curvature relationship it is necessary to extract the curvature from the trajectory of the walker. The radius of curvature is usually calculated by use of the formula:

$$R(t) = \left(\dot{x}^2 + \dot{y}^2\right)^{3/2} / (\dot{x} \cdot \ddot{y} - \dot{y} \cdot \ddot{x}) \tag{5}$$

where $\dot{x}$, $\ddot{x}$, $\dot{y}$ and $\ddot{y}$ are the first and second time derivatives, respectively, of the x and y coordinates of the subject's position in space. This method will be called the *actual path method* or APM. Unfortunately, calculation of the curvature from the subject's trajectory using this formula amplifies the noise inherent in the measurement process and therefore requires a large amount of filtering (cut-off frequency 0.5 Hz). For this reason a second way of measuring the path was developed in which the curvature of the template on the ground closest to the subject was used. This will be called the *ideal path method*.

Ideal path method

At each instant, the ideal path method (IPM) consists in establishing a correspondence between each point on the actual path (trajectory of the walker) with a corresponding point on the ideal path drawn on the ground. For our given recorded position of the body, we calculated the equations of the perpendicular to the tangent line to the body trajectory. This line intersects at a given point with the ideal path for which the curvature is known exactly through Eqs. (3) and (4). The IPM therefore avoids the filtering required for the APM. An illustration of the application of this technique is given for both the whole shape and specific portions of the path (Fig. 3).

Velocity/curvature relation

After filtering, the first and last ten percent of the data (filtered velocity and actual curvature profiles, and also the unfiltered ideal curvature profile) for each completion of the shape were discarded to eliminate distortions from digital filter onsets (Schaal and Sternad 2001). The velocity profile of the body was then compared to both the curvature profile generated by the actual and ideal path methods (Fig. 4).

Statistical analysis

Every statistical test was performed on the Fisher transform of the correlation coefficients rather than directly on the correlation coefficients themselves. However, in the results section, the values were transformed back and reported into their original scale. Not only were the correlation coefficients compared (9 subjects×2 methods×3 laps×2 loops for the limacon) but also the slopes of the regression line β and the velocity gain factors K using repeated measurements analysis of variance (ANOVA) and t tests by means of the Statistica 5.1 software package (Statsoft).

Results

Body trajectories and imposed paths

As a first observation it was noted that at the regions of highest curvature the recorded trajectories of the body projected on to the floor were inside the template drawn on the ground (Fig. 2). Given that the measured position is the midpoint between the shoulders and that the experimenter carefully monitored that the feet were on the shape, this observation reveals a tendency for subjects to lean inside the curve when performing the task. This effect of leaning was strongest in regions of highest curvature and is therefore consistent with the countering of centrifugal force with gravity to maintain balance. The upper-body trajectories (actual path) are therefore not completely superimposable on the templates (ideal path) drawn on the floor.

To obtain a measure of this disparity the average curvature per lap and per loop for the ideal and actual paths were calculated. The mean radius of curvature is 1.25 m for the ideal cloverleaf whereas it is 1.19±0.08 m (across subjects) for the actual path. No significant difference was observed across trials or laps (P>.05) nor between the actual and ideal paths for the mean radius of curvature (P>.05). The mean radius of curvature was equal to 2.18 m for the small loop and 2.98 m for the big loop of the ideal limacon. These values were equal to 1.95±0.27 and 3.15±0.23 m (across subjects), respectively, for the small and big loops of the actual path. No significant difference was observed across trials or across laps

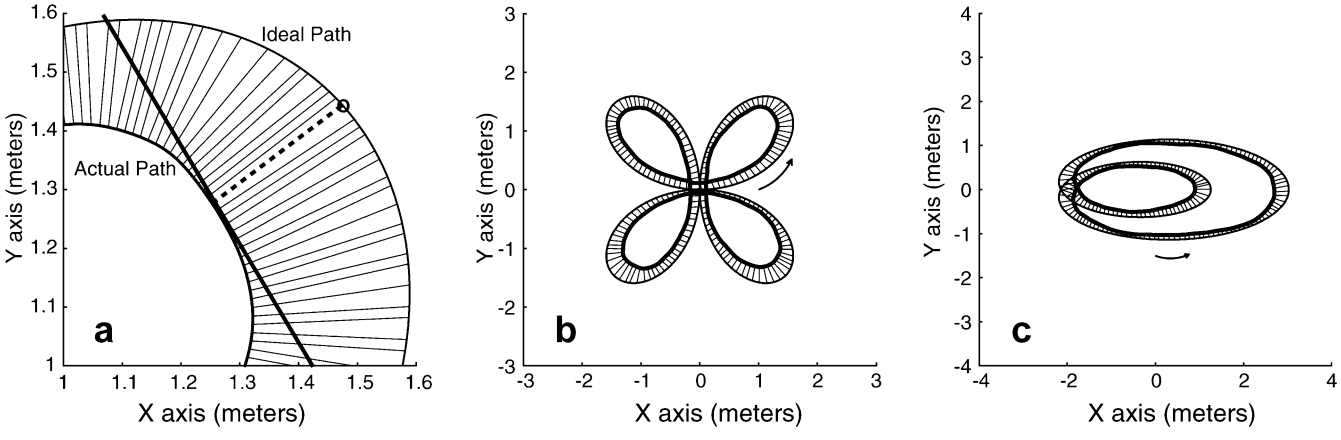

Fig. 3 (*Left panel*) Local correspondence. Illustration of the technique developed to establish a correspondence between shape points and body positions. For each recorded position on the actual body path we look for the intersection point between the perpendicular (*dashed line*) to the tangent line (*solid line*) and the shape to be followed, considered the "ideal" path. At this intersection point with the shape (*open circle*), the corresponding radius of curvature is calculated. (*Middle and right panels*) Whole shape correspondence. Calculation of the curvature from the shape to be followed. For each position of the body projected on the ground (*dark line, inside*) a corresponding point is chosen on the shape to be followed (*clear line, outside*). Although we performed calculations with the totality of the segments linking each point of the actual path to a corresponding point of the ideal path, we display here only quarter segments for reasons of clarity

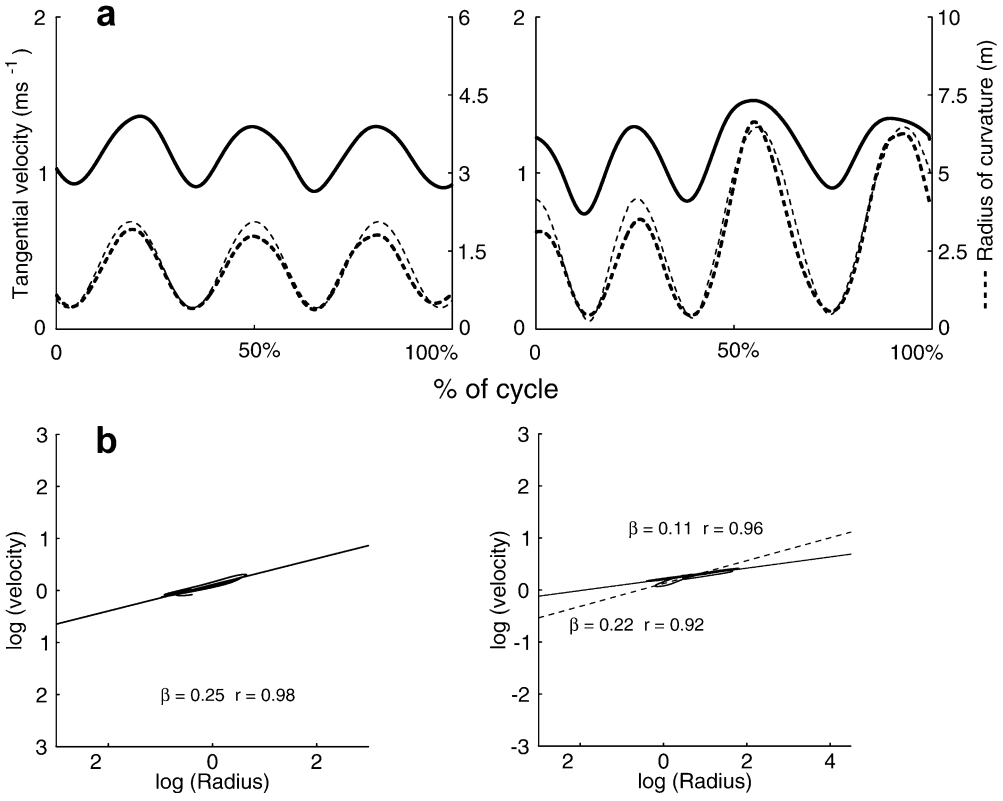

Fig. 4 Velocity–curvature relationship for a typical subject. *Left*, cloverleaf; *right*, limacon. *Top panel*: Time course of the body velocity (*bold line*), and radius of curvature (*dashed fee*) for both actual (*bold*) and ideal (*thin*) paths. The time course presented corresponds to a complete revolution (cycle) of the shape. *Bottom panel*: power law between the velocity and the radius of curvature in a log–log scale (the *right plot* corresponds to the two loops of the limacon)

(*P*>.05) for each loop of the limacon. No significant difference was observed between the actual and ideal paths when comparing each loop of the actual path with the corresponding loop of the ideal path (*P*>.05). However, for the cloverleaf and for the small loop of the limacon, the mean curvature of the ideal path was slightly higher than that of the actual path. This is explained by the observation that regions of highest curvature of the actual trajectories are usually within the ideal ones (Fig. 2).

Rhythm of execution

The average velocities over shape completions were equal to 1.09±0.10 m s^{-1} for the cloverleaf and 1.24±0.11 m s^{-1} for the limacon (no significant difference across successive completions or laps, *P*>.05). These average velocities were statistically different between the two shapes ($F_{(1,6)}$=119.42, *P*<.0001). Interestingly, the average distances covered by subjects were also statistically different between the two shapes (16.42±0.94 m for the cloverleaf and 17.60±0.68 m for the limacon, $F_{(1,6)}$=107.86, *P*<.0001). As a result, a tendency for all subjects to maintain a constant duration for the completion of a movement cycle was observed even if these durations were statistically different between each shape (15.30 ±1.97 s for the cloverleaf and 14.33±1.65 s for the limacon —$F_{(1,6)}$=19.41, *P*<.01).

Speed–radius relationship: actual and ideal path

The velocity–curvature relationship is expressed here using a logarithmic scale (Eq. 2) to identify any dependencies given by a power law. The results were analysed in three stages: first the existence of a strong correlation between velocity and curvature was tested (by calculating the *r* correlation coefficient between these variables). Then the slopes of the regression line which gives the power-law exponent β and the velocity gain factor *K* (Eq. 2) were calculated. All of these results (*r* coefficient and terms of the power law) are presented for the two methods of curvature calculation (APM or IPM; Tables 1 and 2).

Concomitant variations of velocity with the geometric aspect of the shape are observed (Fig. 4) in the form of a strong relationship between the tangential velocity and the radius of curvature (for both actual and ideal paths) expressed in a logarithmic scale (Fig. 4). This relation is well described by a power law.

The results are presented for each subject and a mean value is also presented across subjects. For each subject we first verified that no significant difference (*P*>.05) was observed between the three performed trials and the three laps within each trial before calculating an average value across the three analyzed trials and the nine corresponding laps.

Table 1 CLOVERLEAF—Correlation Coefficients (r) and Slopes of the regression line (β) between log V and log R (actual and ideal paths) for all subjects. No difference (P>.05) is observed between successive laps (repetitions) for each subject. The mean results and standard deviation across subjects are also presented

	Actual path		Ideal path	
	r	β	r	β
S1	0.96	0.26	0.91	0.25
S2	0.97	0.23	0.95	0.26
S3	0.96	0.24	0.91	0.22
S4	0.92	0.20	0.89	0.20
S5	0.96	0.24	0.96	0.29
S6	0.96	0.24	0.96	0.28
S7	0.98	0.30	0.94	0.29
S8	0.98	0.28	0.96	0.29
S9	0.98	0.30	0.93	0.28
Mean	0.96±0.03	0.25±0.04	0.93±0.03	0.26±0.04

Table 2 LIMACON—correlation coefficients (r) and Slopes of the regression line (β) between log V and log R (actual and ideal paths) for all subjects. No difference (P>.05) is observed between successive laps (or loops) for each subject. The mean results and standard deviation across subjects are also presented

	Actual path				Ideal path			
	Small loop		Big loop		Small loop		Big loop	
	r	β	r	β	r	β	r	β
S1	0.93	0.23	0.96	0.12	0.84	0.12	0.92	0.10
S2	0.94	0.28	0.97	0.17	0.88	0.18	0.93	0.13
S3	0.90	0.23	0.91	0.13	0.90	0.14	0.91	0.10
S4	0.93	0.20	0.95	0.13	0.91	0.16	0.93	0.12
S5	0.93	0.24	0.95	0.19	0.92	0.18	0.97	0.15
S6	0.93	0.28	0.95	0.16	0.96	0.21	0.92	0.15
S7	0.91	0.31	0.97	0.18	0.89	0.20	0.93	0.15
S8	0.93	0.27	0.96	0.17	0.93	0.19	0.95	0.14
S9	0.94	0.32	0.95	0.18	0.91	0.19	0.93	0.15
Mean	0.92 ±0.08	0.26 ±0.07	0.95 ±0.04	0.16 ±0.03	0.91 ±0.04	0.17 ±0.03	0.93 ±0.03	0.13 ±0.02

Cloverleaf

The strength of the velocity–curvature correlation For the cloverleaf the correlation coefficients between log V and log R were always higher than 0.80 for all subjects for both ideal and actual paths. On average this correlation coefficient was equal to 0.96±0.03 for the actual path and 0.93±0.03 for the ideal path.

The velocity gain factor K This quantity relates the geometrical and kinematic aspects of the movement trajectory, either at the level of the shape as a whole or within segments of the shape. Strong variability was observed between the subjects, explained by their different natural walking speeds. The mean log K across subjects was equal to 0.04±0.10 (actual path) and 0.01±0.09 (ideal path) for a complete lap. The K values are not significantly different between the actual path and the ideal path (P>.05).

The exponent β of the measured power law Again, the slopes of the regression line β between log V and log R were not significantly different for the actual (0.25±0.04) versus the ideal (0.26±0.04) paths (P>.05). The exponent β ranged between 0.20 and 0.29 for the ideal path and between 0.20 and 0.30 for the actual path. It can already be observed that for the cloverleaf the exponent is systematically less than the one-third value seen in hand drawing and for locomotion around an ellipse (Vieilledent et al. 2001). For drawing, Viviani and Flash reported for the cloverleaf, a mean β value of 0.325 (β ranged between 0.287 and 0.391 for the three subjects which participated in their experiments).

Limacon

The strength of the velocity–curvature correlation The correlation coefficient between log V and log R is equal to 0.92±0.08 and 0.95±0.04 for the actual path and 0.91±0.04 and 0.93±0.03 for the ideal path, respectively, for the small and large loops of the limacon.

The velocity gain factor K We observed a strong modulation of K between the small (log K=−0.001 ±0.091 and 0.002±0.097, respectively, for the actual and ideal path) and large (log K=0.13±0.10 and 0.12±0.09, respectively, for the actual and ideal path) loops of the limacon. K values are not different for the actual and the ideal paths (P>.05). Thus clear modulation the velocity gain factor is observed here (unlike for the loops of the cloverleaf) at the transition point separating the two subunits of the limacon ($F_{(1,7)}$=264.12, P<.0001 for the actual path, and $F_{(1,7)}$=508.43, P<.0001 for the ideal path). The same observations (a single K value for the cloverleaf and different K values for the two loops of the limacon) were reported by Viviani and Flash for hand drawing movements.

The exponent β of the measured power law For the limacon β was equal to 0.26±0.07 and 0.16±0.03 respectively for the small and large loops of the actual path and was equal to 0.17±0.03 and 0.13±0.02 for the same loops of the ideal path. These results show a significant difference between the actual and the ideal paths ($F_{(1,7)}$=35.53; P<.01) which is also observed when the small and large loops of either the actual path ($F_{(1,7)}$=89.78; P<.001) or the ideal path ($F_{(1,7)}$=77.20; P<.001) are compared. It is clear for the limacon that two different β values are observed, one for each portion (loop) of the shape. Again, our results for locomotion are different (much lower) from those reported by Viviani and Flash (1995) for the same shape studied in hand drawing. The last authors reported mean β values of 0.340 (β ranged between 0.324 and 0.357) and 0.321 (β ranged between 0.310 and 0.329), respectively, for the small and large loops of the limacon. While these authors found only a modulation of the K factor we report here also a modulation of the β exponent.

The variability of the results is greater when using the APM compared to the IPM for the limacon.

Velocity/curvature—influence of the magnitude of curvature

It was noted earlier that the trajectory of the upper body (actual path) was often within the position of the shape drawn on the ground revealing the need of the walker to lean inside the curve to perform the task correctly. The function of leaning is probably to allow the walker to compensate for the centrifugal acceleration (mV^2/R) as suggested by Greene (1985) in a study where subjects had to run at a maximum velocity along an arc of circle. Because this mechanical effect is one possible explanation for the velocity–curvature relationship in locomotion, we tested how important the magnitude of curvature of the actual path is on the resulting velocity-curvature relationship for human walking. To this purpose we performed a sub-analysis to investigate the characteristics of the velocity–curvature relationship for the same magnitude of curvature (for a radius less than 2.01 m) for the two geometrical forms (Fig. 4). This tests if the form of the local–velocity curvature relationship is context dependent, i.e. depends on the global geometrical form of the shape. For this analysis, we also verified how repetitive and homogeneous our experimental observations were across trials (n=27 for each shape), by verifying that no statistically significant difference exists from one trial to another (P>.05).

Cloverleaf and limacon

The mean correlation coefficients between log V and log R were equal to 0.96±0.03 for the cloverleaf and were 0.89 ±0.13 and 0.82±0.15, respectively, for the small and large loop of the limacon.

Although we are examining here the two loops of the limacon within a similar magnitude of curvature, the velocity gain factor was statistically different for the two loops of the shape ($F_{(1,7)}$=252.09; P<.001). Mean K values were equal to −0.007±0.104 and 0.13±0.09, respectively, for the small and large loops of the limacon, and comparable with the results obtained for the "entire shape" analysis previously presented. The mean log K value for the cloverleaf is similar to that observed for the same shape before (0.05±0.10).

Again, β values are comparable with the results presented in the previous section. Mean β values were equal to 0.26±0.04 for the cloverleaf and equal to 0.28 ±0.11 and 0.13±0.03, respectively, for the small and large loops of the limacon. A statistically significant difference was observed between these loops ($F_{(1,7)}$=147.73; P<.001).

This analysis demonstrates that the relationship between the instantaneous velocity and curvature does depend on context (the exponents were 0.26, 0.28, and 0.13). Hence, the form of the local relationship is a function of more global aspects of the shape.

Discussion

The existence of a close relationship between the instantaneous velocity of the body and the instantaneous curvature of the shape was seen in a previous study (Vieilledent et al 2001) in which subjects were required to walk around ellipses of various size drawn on the ground. This relationship was well described by the one-third power law, which has been seen in the drawing of shapes by the hand. This result raised the intriguing possibility that some of the geometrical aspects of locomotor and hand-movement planning might be shared. However, the ellipse is a special case for the one-third power law, and hence if the result is to be established as general principle of locomotion around curved paths more complex shapes should be tested. This was the aim of the present study in which walking of the cloverleaf and limacon was examined.

In contrast with the study of elliptical paths, our results demonstrate that the one-third power law does not describe the velocity–curvature relationship in locomotion around more complex shapes. Although this relationship can still be described by a power law, the exponent is no longer fixed at the 0.33 value but is a function of the shape. The values are not in agreement with those reported for the drawing of the same shapes (Viviani and Flash 1995).

Another aspect of the one-third power law is its use in the inference of segmented planning by the central nervous system. In hand movements a pre-factor in the law, the velocity gain factor K, is seen to change at different segments of the paths (Viviani and Cenzato 1985). The shapes chosen here allowed us to test this aspect of locomotion by examination of the modulation of the terms of the power-law fit around different portions of the shape. For locomotion along these shapes, both the velocity gain factor K and the power law exponent β were seen to be modulated at the transitions points separating two subunits of the trajectory. This type of description of the trajectory by the power law is more in the nature of a fit of a function to data rather than a general principle—the power law does not describe locomotion with the same level of generality as for hand movements. Irrespective of the form of the law relating velocity to curvature, our results show that even for complex shapes the velocity varies with instantaneous curvature. However the form of this relationship does not seem to be constant over shapes. This curious fact suggests that both local and global geometric aspects are taken into account in the planning strategy—velocity is always a function of local curvature but the function changes with the global aspects of the shape.

One question raised in this study, which is also applicable to the tracing of shapes by the hand, is which properties of the trajectory to use in the calculation of the curvature variable from the data. Two paths can be used in

the calculation of curvature—the actual path chosen by the walker or the template drawn on the ground. Although similar, they were not identical, because it was noted that the actual path was often within the ideal path, because of the lean of the walker. In examining velocity–curvature relationships it can be asked whether the velocity variations were related to the variations of curvature of the actual or ideal path. The quantitative differences in the power law terms observed between the actual and ideal paths might be attributed to the methods used for calculating curvature (the APM might give different results, depending on the filtering algorithms, see Schaal and Sternad 2001). However, we found that the global features of the velocity–curvature relationship are similarly observed (a strong correlation, the K factor is unchanged from one loop of the cloverleaf to another, the K factor and the β exponent changing from one loop of the limacon to another) for the ideal and actual paths. However, with the ideal path method, it is possible to relate velocity profiles (which differ across subjects) to a single geometrical form, i.e. the ideal path along which subjects had to walk. Furthermore, this method relies on a simple geometrical transformation (a projection from one path to another) and is not sensitive to the properties of filtering algorithms used to calculate curvature. Thus, for studies where the geometrical form of the path is constrained, investigating the influence of the curvature variations of the imposed (ideal) path on the kinematic profile would be advantageous, because it avoids filtering. It can also be argued that the ideal path is the goal of the walker and therefore a source of information taken into consideration by subjects. In a study that examined the anticipative control of car driving, the driver knows before taking a bend that he will have to decelerate at the point of maximum curvature (Land and Lee 1994). The same type of problem between the geometry and kinematics must be solved by the CNS—both visual information and knowledge about the locomotor apparatus (Loomis and Beall 1998) might interact during walking enabling humans to control their movement. During locomotion along curved trajectories, "perceptuo-locomotor" interactions comparable with the "perceptuo-motor" interactions described by Viviani et Stucchi (1989, 1992) are likely to be part of the planning strategies. This proposal of perceptuo-locomotor interactions in relation to the velocity–curvature relationship is compatible with recent results obtained by Reina et Schwartz (2003). They provided some evidence for kinematic coupling of eye and hand movements in a task in which monkeys had to draw ellipses in a free space. They found that saccades occurred just before the hand had moved into the subsequent segment of the path and fixated near the point of maximum curvature. Because the hand movement was found to obey the power law, the authors proposed that the eye motion planning was carried out in accordance with the hand planning strategy. It is possible that comparable coupling between eye and body movements exists for locomotion. The recording of eye movements during locomotion around large and curved paths might help to answer the question of the nature of the path being considered by subjects in order to modulate their velocity profile.

In the examination of the actual (position of the upper body) and ideal (position of the feet) paths it was noted that the subjects had a tendency to lean into the curve, particularly at points of high curvature. As has been previously mentioned this suggests the need to balance the outward centrifugal effects of turning with the inward force of gravity projected through the angled body. This is a potential explanation of the local nature of the velocity–curvature relationship; it does not, however, describe the global modulation. Further investigation and modelling is necessary to produce a testable hypothesis that examines the extent to which the velocity–curvature relationship can be explained either by purely mechanical relations, centrally generated planning strategies, or some combination thereof.

Acknowledgements The authors wish to thank S. Dalbera and T. Ducourant for their technical assistance during the experiments and F. Maloumian for the graphs. This study was supported by a grant "Cognitique Thème Action" from the French Ministry of Research (MENRT).

References

Abend W, Bizzi E, Morasso P (1982) Human arm trajectory formation. Brain 105:331–348

Cavagna GA, Margaria R (1966) Mechanics of walking. J Appl Physiol 21:271–278

Cheron G, Draye JP, Bengoetxea A, Dan B (1999) Kinematics invariance in multi-directional complex movements in free space: effect of changing direction. Clin Neurophysiol 110:757–764

Courtine G, Schieppati M (2003) Human walking along a curved path. I. Body trajectory, segment orientation and the effect of vision. Eur J Neurosci 18:177–190

de'Sperati C, Viviani P (1997) The relationship between curvature and velocity in two-dimensional smooth pursuit eye movements. J Neurosci 17:3932–3945

Flash T, Hogan N (1985) The coordination of arm movements: An experimentally confirmed mathematical model. J Neurosci 5:1688–1703

Grasso R, Glasauer S, Takei Y, Berthoz A (1996) The predictive brain: anticipatory control of head direction for the steering of locomotion. Neuroreport 7:1170–1174

Grasso R, Prevost P, Ivanenko YP, Berthoz A (1998) Eye-head coordination for the steering of locomotion in humans : an anticipatory strategy. Neurosci Lett 253:115–118

Greene PR (1985) Running on flat turns : experiments, theory, and applications. J Biomech Eng 107:96–103

Gribble PL, Ostry DJ (1996) Origins of the power law relation between movement velocity and curvature: modeling the effects of muscle mechanics and limb dynamics. J Neurophysiol 76:2853–2860

Harris MH, Wolpert DM (1998) Signal-dependant noise determines motor planning. Nature 394:780–784

Imai T, Moore ST, Raphan T, Cohen B (2001) Interaction of body, head, and eyes during walking and turning. Exp Brain Res 136:1–18

Ivanenko YP, Grasso R, Macellari V, Lacquaniti F (2002) Two-thirds power law in human locomotion: role of ground contact forces. Neuroreport 13:1171–1174

Kawato M, Maeda Y, Uno Y, Suzuki R (1990) Trajectory formation of arm movement by cascade neural network model based on minimum torque-change criterion. Biol Cyber 62:275–288

Lacquaniti F, Terzuolo C, Viviani P (1983) The law relating the kinematic and figural aspects of drawing movements. Acta Psychol 54:115–130

Land MF, Lee DN (1994) Where we look when we steer. Nature 369:742–744

Loomis JM, Beall AC (1998) Visually controlled locomotion: its dependence on optic flow, three-dimensional space perception, and cognition. Ecol Psychol 10:271–285

Massey JT, Lurito JT, Pellizzer G, Georgopoulos AP (1992) Three-dimensional drawings in isometric conditions: relation between geometry and kinematics. Exp Brain Res 88:685–690

Reina GA, Schwartz AB (2003) Eye-hand coupling during closed-loop drawing: evidence of shared motor planning? Hum Mov Sci 22:137–152

Richardson MJ, Flash T (2002) Comparing smooth arm movements with the two-thirds power law and the related segmented-control hypothesis. J Neurosci 22:8201–8211

Schaal S, Sternad D (2001) Origins and violations of the 2/3 power law in rhythmic three-dimensional arm movements. Exp Brain Res 136:60–72

Schwartz AB, Moran DW (1999) Motor cortical activity during drawing movements : population representation during lemniscate tracing. J Neurophysiol 82:2705–2718

Sternad D, Schaal S (1999) Segmentation of endpoint trajectories does not imply segmented control. Exp Brain Res 124:118–136

Todorov E, Jordan MI (1998) Smoothness maximization along a predefined path accurately predicts the speed profiles of complex arm movements. J Neurophysiol 80:696–714

Vieilledent S, Kerlirzin Y, Dalbera S, Berthoz A (2001) Relationship between velocity and curvature of a locomotor trajectory in human. Neurosci Lett 305:65–69

Viviani P, Cenzato M (1985) Segmentation and coupling in complex movements. J Exp Psychol Hum Percep Perf 11:828–845

Viviani P, Flash T (1995) Minimum-jerk, two-thirds power law, and isochrony: converging approaches to movement planning. J Exp Psychol Hum Percep Perf 21:32–53

Viviani P, Stucchi N (1989) The effect of movement velocity on form perception: geometric illusions in dynamic displays. Percept Psychophys 46:266–274

Viviani P, Stucchi N (1992) Biological movements look uniform: evidence of motor-perceptual interactions. J Exp Psychol Hum Percep Perf 18:603–623

Viviani P, Terzuolo C (1982) Trajectory determines movement dynamics. Neuroscience 7:431–437

Wann JP, Nimmo-Smith I, Wing AM (1988) Relation between velocity and curvature in movement: equivalence and divergence between a power law and a minimum-jerk model. J Exp Psychol Hum Percep Perf 14:622–637

Warren WH, Kay BA, Zosh WD, Duchon AP, Sahuc S (2001) Optic flow is used to control human walking. Nat Neurosci 4:213–216

Wilkie RM, Wann JP (2003) Eye-movements aid the control of locomotion. J Vision 3:1–9

Willems PA, Cavagna GA, Heglund NC (1995) External, internal and total work in human locomotion. J Exp Biol 198:379–393